Pergamon

Carbon, Vol. 33, No. 7, pp. 873–881, 1995

0008-6223/95 $9.50 + .00

0008-6223(95)00016-X

PYROLYTIC CARBON NANOTUBES FROM VAPOR-GROWN CARBON FIBERS

MORINOBU ENDO,[1] KENJI TAKEUCHI,[1] KIYOHARU KOBORI,[1] KATSUSHI TAKAHASHI,[1] HAROLD W. KROTO,[2] and A. SARKAR[2]

[1]Faculty of Engineering, Shinshu University, 500 Wakasato, Nagano 380, Japan
[2]School of Chemistry and Molecular Sciences, University of Sussex, Brighton BN1 9QJ, U.K.

(*Received* 21 *November* 1994; *accepted* 10 *February* 1995)

Abstract—The structure of as-grown and heat-treated pyrolytic carbon nanotubes (PCNTs) produced by hydrocarbon pyrolysis are discussed on the basis of a possible growth process. The structures are compared with those of nanotubes obtained by the arc method (ACNT; arc-formed carbon nanotubes). PCNTs, with and without secondary pyrolytic deposition (which results in diameter increase) are found to form during pyrolysis of benzene at temperatures ca. 1060°C under hydrogen. PCNTs after heat treatment at above 2800°C under argon exhibit have improved stability and can be studied by high-resolution transmission electron microscopy (HRTEM). The microstructures of PCNTs closely resemble those of vapor-grown carbon fibers (VGCFs). Some VGCFs that have micro-sized diameters appear to have nanotube inner cross-sections that have different mechanical properties from those of the outer pyrolytic sections. PCNTs initially appear to grow as ultra-thin graphene tubes with central hollow cores (diameter ca. 2 nm or more) and catalytic particles are not observed at the tip of these tubes. The secondary pyrolytic deposition, which results in characteristic thickening by addition of extra cylindrical carbon layers, appears to occur simultaneously with nanotube lengthening growth. After heat treatment, HRTEM studies indicate clearly that the hollow cores are closed at the ends of polygonized hemi-spherical carbon caps. The most commonly observed cone angle at the tip is generally ca. 20°, which implies the presence of five pentagonal disclinations clustered near the tip of the hexagonal network. A structural model is proposed for PCNTs observed to have spindle-like shape and conical caps at both ends. Evidence is presented for the formation, during heat treatment, of hemi-toroidal rims linking adjacent concentric walls in PCNTs. A possible growth mechanism for PCNTs, in which the tip of the tube is the active reaction site, is proposed.

Key Words—Carbon nanotubes, vapor-grown carbon fibers, high-resolution transmission electron microscope, graphite structure, nanotube growth mechanism, toroidal network.

1. INTRODUCTION

Since Iijima's original report[1], carbon nanotubes have been recognized as fascinating materials with nanometer dimensions promising exciting new areas of carbon chemistry and physics. From the viewpoint of fullerene science they also are interesting because they are forms of giant fullerenes[2]. The nanotubes prepared in a dc arc discharge using graphite electrodes at temperatures greater than 3000°C under helium were first reported by Iijima[1] and later by Ebbesen and Ajyayan[3]. Similar tubes, which we call pyrolytic carbon nanotubes (PCNTs), are produced by pyrolyzing hydrocarbons (e.g., benzene at ca. 1100°C)[4–9]. PCNTs can also be prepared using the same equipment as that used for the production of so called vapor-grown carbon fibers (VGCFs)[10]. The VGCFs are micron diameter fibers with circular cross-sections and central hollow cores with diameters ca. a few tens of nanometers. The graphitic networks are arranged in concentric cylinders. The intrinsic structures are rather like that of the annual growth of trees. The structure of VGCFs, especially those with hollow cores, are very similar to the structure of arc-formed carbon nanotubes (ACNTs). Both types of nanotubes, the ACNTs and the present PCNTs, appear to be essentially Russian Doll-like sets of elongated giant fullerenes[11,12]. Possible growth processes have been proposed involving both open-ended[13] and closed-cap[11,12] mechanisms for the primary tubules. Whether either of these mechanisms or some other occurs remains to be determined.

It is interesting to compare the formation process of fibrous forms of carbon with larger micron diameters and carbon nanotubes with nanometer diameters from the viewpoint of "one-dimensional" carbon structures as shown in Fig. 1. The first class consists of graphite whiskers and ACNTs produced by arc methods, whereas the second encompasses vapor-grown carbon fibers and PCNTs produced by pyrolytic processes. A third possible class would be polymer-based nanotubes and fibers such as PAN-based carbon fibers, which have yet to be formed with nanometer dimensions. In the present paper we compare and discuss the structures of PCNTs and VGCFs.

2. VAPOR-GROWN CARBON FIBERS AND PYROLYTIC CARBON NANOTUBES

Vapor-grown carbon fibers have been prepared by catalyzed carbonization of aromatic carbon species using ultra-fine metal particles, such as iron. The particles, with diameters less than 10 nm may be dispersed on a substrate (substrate method), or allowed to float in the reaction chamber (fluidized method). Both

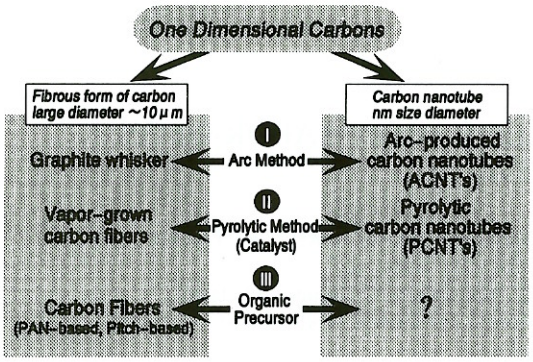

Fig. 1. Comparative preparation methods for micrometer size fibrous carbon and carbon nanotubes as one-dimensional forms of carbon.

methods give similar structures, in which ultra-fine catalytic particles are encapsulated in the tubule tips (Fig. 2). Continued pyrolytic deposition occurs on the initially formed thin carbon fibers causing thickening (ca. 10 μm diameter, Fig. 3a). Substrate catalyzed fibers tend to be thicker and the floating technique produces thinner fibers (ca. 1 μm diameter). This is due to the shorter reaction time that occurs in the fluidized method (Fig. 3b). Later floating catalytic methods are useful for large-scale fiber production and, thus, VGCFs should offer a most cost-effective means of producing discontinuous carbon fibers. These VGCFs offer great promise as valuable functional carbon filler materials and should also be useful in carbon fiber-reinforced plastic (CFRP) production. As seen in Fig. 3b even in the "as-grown" state, carbon particles are eliminated by controlling the reaction conditions. This promises the possibility of producing pure ACNTs without the need for separating spheroidal carbon particles. Hitherto, large amounts of carbon particles have always been a byproduct of nanotube production and, so far, they have only been eliminated by selective oxidation[14]. This has led to the loss of significant amounts of nanotubes—ca. 99%.

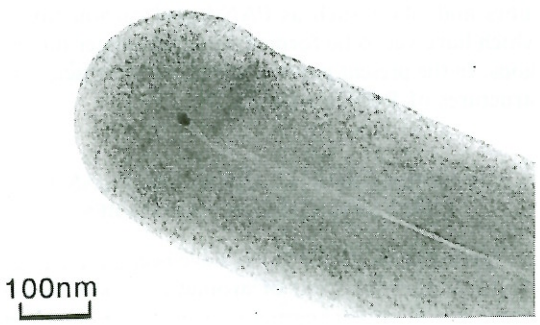

Fig. 2. Vapour-grown carbon fiber showing relatively early stage of growth; at the tip the seeded Fe catalytic particle is encapsulated.

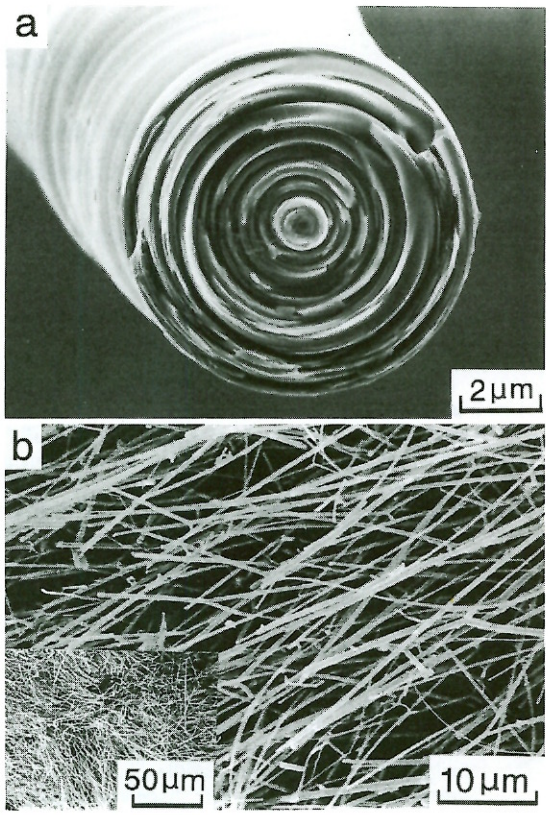

Fig. 3. Vapor-grown carbon fibers obtained by substrate method with diameter ca. 10 μm (a) and those by floating catalyst method (b) (inserted, low magnification).

3. PREPARATION OF VGCFs AND PCNTs

The PCNTs in this study were prepared using the same apparatus[9] as that employed to produce VGCFs by the substrate method[10,15]. Benzene vapor was introduced, together with hydrogen, into a ceramic reaction tube in which the substrate consisted of a centrally placed artificial graphite rod. The temperature of the furnace was maintained in the 1000°C range. The partial pressure of benzene was adjusted to be much lower than that generally used for the preparation of VGCFs[10,15] and, after one hour decomposition, the furnace was allowed to attain room temperature and the hydrogen was replaced by argon. After taking out the substrate, its surface was scratched with a toothpick to collect the minute fibers. Subsequently, the nanotubes and nanoscale fibers were heat treated in a carbon resistance furnace under argon at temperatures in the range 2500–3000°C for ca. 10–15 minutes. These as-grown and sequentially heat-treated PCNTs were set on an electron microscope grid for observation directly by HRTEM at 400kV acceleration voltage.

It has been observed that occasionally nanometer scale VGCFs and PCNTs coexist during the early stages of VGCF processing (Fig. 4). The former tend to have rather large hollow cores, thick tube walls and well-organized graphite layers. On the other hand,

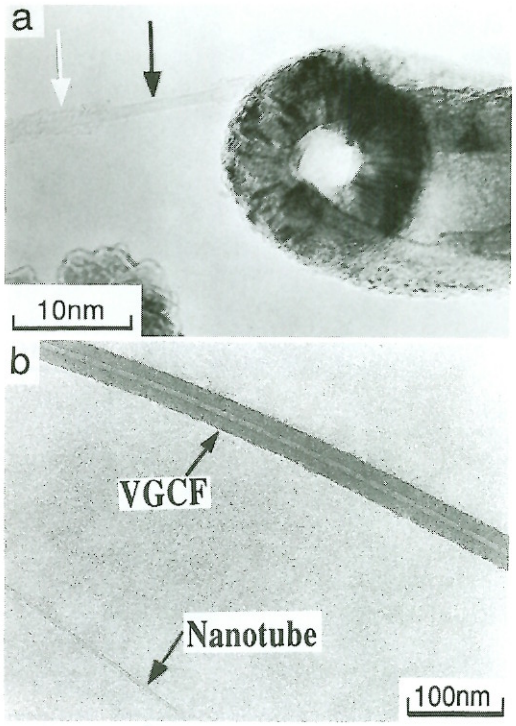

Fig. 4. Coexisting vapour-grown carbon fiber, with thicker diameter and hollow core, and carbon nanotubes, with thinner hollow core, (as-grown samples).

PCNTs tend to have very thin walls consisting of only a few graphitic cylinders. Some sections of the outer surfaces of the thin PCNTs are bare, whereas other sections are covered with amorphous carbon deposits (as is arrowed region in Fig. 4a). TEM images of the tips of the PCNTs show no evidence of electron beam opaque metal particles as is generally observed for VGCF tips[10,15]. The large size of the cores and the presence of opaque particles at the tip of VGCFs suggests possible differences between the growth mechanism for PCNTs and standard VGCFs[7–9]. The yield of PCNTs increases as the temperature and the benzene partial pressure are reduced below the optimum for VGCF production (i.e., temperature ca. 1000°–1150°C). The latter conditions could be effective in the prevention or the minimization of carbon deposition on the primary formed nanotubules.

4. STRUCTURES OF PCNTs

Part of a typical PCNT (ca. 2.4 nm diameter) after heat treatment at 2800°C for 15 minutes is shown in Fig. 5. It consists of a long concentric graphite tube with interlayer spacings ca. 0.34 nm – very similar in morphology to ACNTs[1,3]. These tubes may be very long, as long as 100 nm or more. It would, thus, appear that PCNTs, after heat treatment at high temperatures, become graphitic nanotubes similar to ACNTs. The heat treatment has the effect of crystallizing the secondary deposited layers, which are usually composed of rather poorly organized turbostratic carbon.

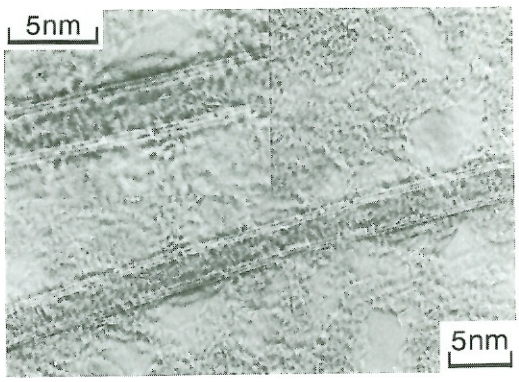

Fig. 5. Heat-treated pyrolytic carbon nanotube and enlarged one (inserted), without deposited carbon.

This results in well-organized multi-walled concentric graphite tubules. The interlayer spacing (0.34 nm) is slightly wider on average than in the case of thick VGCFs treated at similar temperatures. This small increase might be due to the high degree of curvature of the narrow diameter nanotubes which appears to prevent perfect 3-dimensional stacking of the graphitic layers[16,17]. PCNTs and VGCFs are distinguishable by the sizes of the well-graphitized domains; cross-sections indicate that the former are characterized by single domains, whereas the latter tend to exhibit multiple domain areas that are small relative to this cross-sectional area. However, the innermost part of some VGCFs (e.g., the example shown in Fig. 5) may often consist of a few well-structured concentric nanotubes. Theoretical studies suggest that this "single grain" aspect of the cross-sections of nanotubes might give rise to quantum effects. Thus, if large scale real-space super-cell concepts are relevant, then Brillouin zone-folding techniques may be applied to the description of dispersion relations for electron and phonon dynamics in these pseudo one-dimensional systems.

A primary nanotube at a very early stage of thickening by pyrolytic carbon deposition is depicted in Figs. 6a–c; these samples were: (a) as-grown and (b), (c) heat treated at 2500°C. The pyrolytic coatings shown are characteristic features of PCNTs produced by the present method. The deposition of extra carbon layers appears to occur more or less simultaneously with nanotube longitudinal growth, resulting in spindle-shaped morphologies. Extended periods of pyrolysis result in tubes that can attain diameters in the micron range (e.g., similar to conventional (thick) VGCFs[10]. Fig. 6c depicts a 002 dark-field image, showing the highly ordered central core and the outer inhomogeneously deposited polycrystalline material (bright spots). It is worthwhile to note that even the very thin walls consisting of several layers are thick enough to register 002 diffraction images though they are weaker than images from deposited crystallites on the tube.

Fig. 7a,b depicts PCNTs with relatively large diameters (ca. 10 nm) that appear to be sufficiently tough

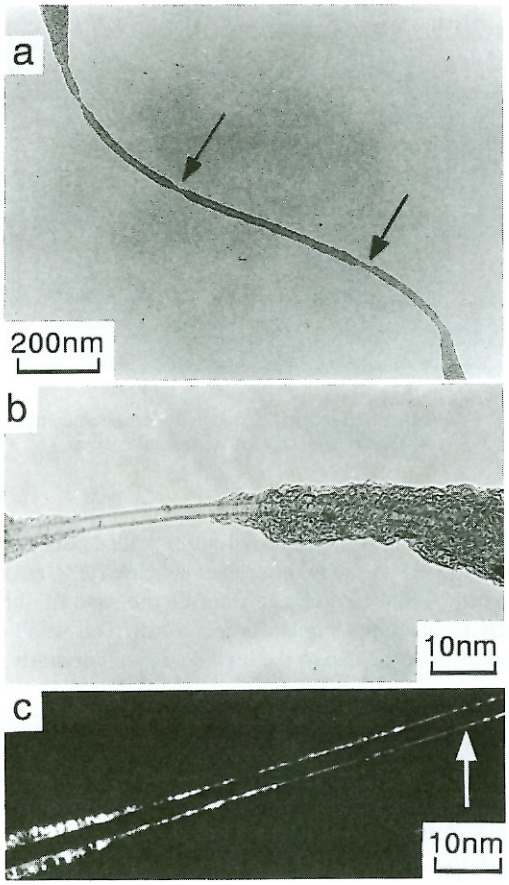

Fig. 6. PCNTs with partially deposited carbon layers (arrow indicates the bare PCNT), (a) as-grown, (b) partially exposed nanotube and (c) 002 dark-field image showing small crystallites on the tube and wall of the tube heat treated at 2500°C.

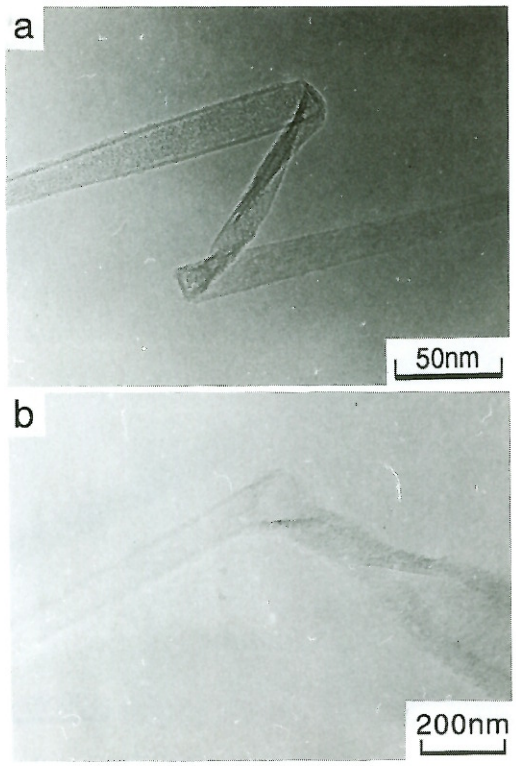

Fig. 7. Bent and twisted PCNT (heat treated at 2500°C).

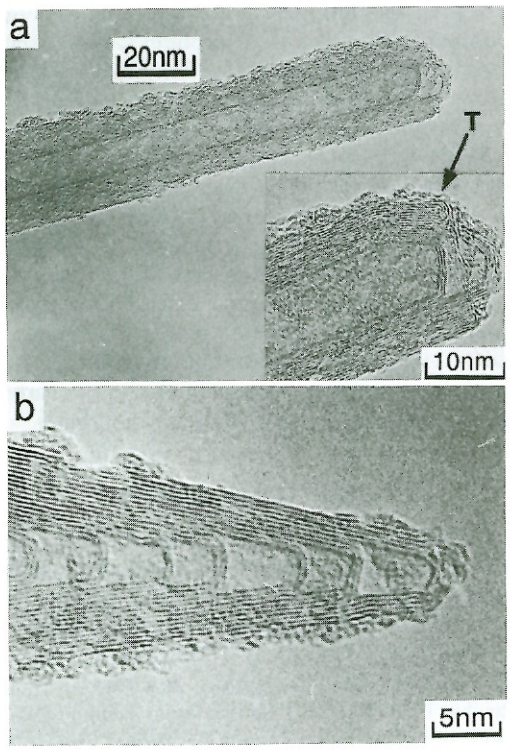

Fig. 8. The tip of PCNTs with continuous hollow core (a) and the cone-like shape (b) (T indicates the toroidal structure shown in detail in Fig. 11).

and flexible to bend, twist, or kink without fracturing. The basic structural features and the associated mechanical behavior of the PCNTs are, thus, very different from those of conventional PAN-based fibers as well as VGCFs, which tend to be fragile and easily broken when bent or twisted. The bendings may occur at propitious points in the graphene tube network[18].

Fig. 8a,b shows two typical types of PCNT tip morphologies. The caps and also intercompartment diaphragms occur at the tips. In general, these consist of 2–3 concentric layers with average interlayer spacing of ca. 0.38 nm. This spacing is somewhat larger than that of the stackings along the radial direction, presumably (as discussed previously) because of sharp curvature effects. As indicated in Fig. 9, the conical shapes have rather symmetric cone-like shells. The angle, ca. 20°, is in good agreement with that expected for a cone constructed from hexagonal graphene sheets containing pentagonal disclinations—as is Fig. 9e. Ge and Sattler[19] have reported nanoscale conical carbon materials with infrastructure explainable on the basis of fullerene concepts. STM measurements show that nanocones, made by deposition of very hot carbon on HOPG surfaces, often tend to

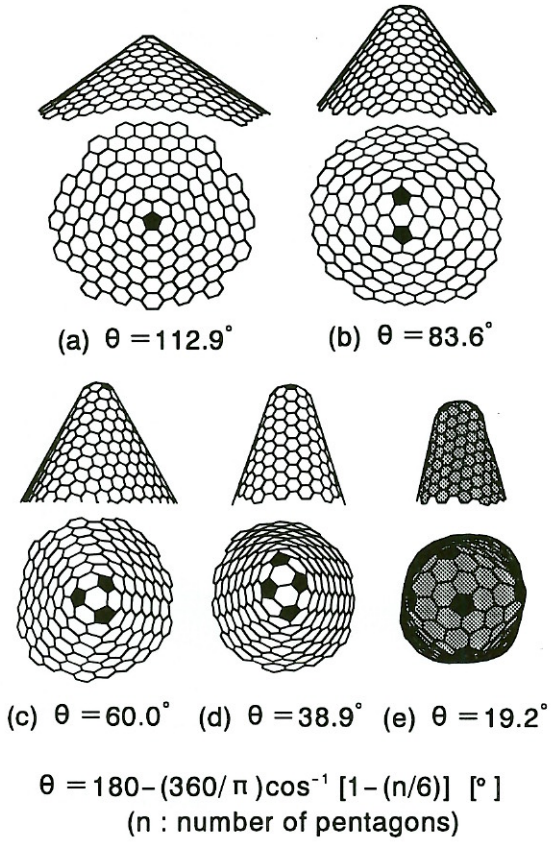

Fig. 9. The possible tip structure with cone shape, in which the pentagons are included. As a function of the number of pentagons, the cone shape changes. The shaded one with 19.2° tip angle is the most frequently observed in PCNTs.

have an opening angle of ca. 20°. Such caps may, however, be of five possible opening angles (e.g., from 112.9° to 19.2°) depending on the number of pentagonal disclinations clustered at the tip of the cone, as indicated in Fig. 9[8]. Hexagons in individual tube walls are, in general, arranged in a helical disposition with variable pitches. It is worth noting that the smallest angle (19.2°) that can involve five pentagons is most frequently observed in such samples. It is frequently observed that PCNTs exhibit a spindle-shaped structure at the tube head, as shown in Fig. 8b.

5. GROWTH MODEL OF PCNTs

In the case of the PCNTs considered here, the growth temperature is much lower than that for ACNTs, and no electric fields, which might influence the growth of ACNTs, are present. It is possible that different growth mechanisms apply to PCNT and ACNT growth and this should be taken into consideration. As mentioned previously, one plausible mechanism for nanotube growth involves the insertion of small carbon species C_n ($n = 1,2,3\ldots$) into a closed fullerene cap (Fig. 10a–c)[11]. Such a mechanism is related to the processes that Ulmer *et al.*[20] and McElvaney *et al.*[21] have discovered for the growth of

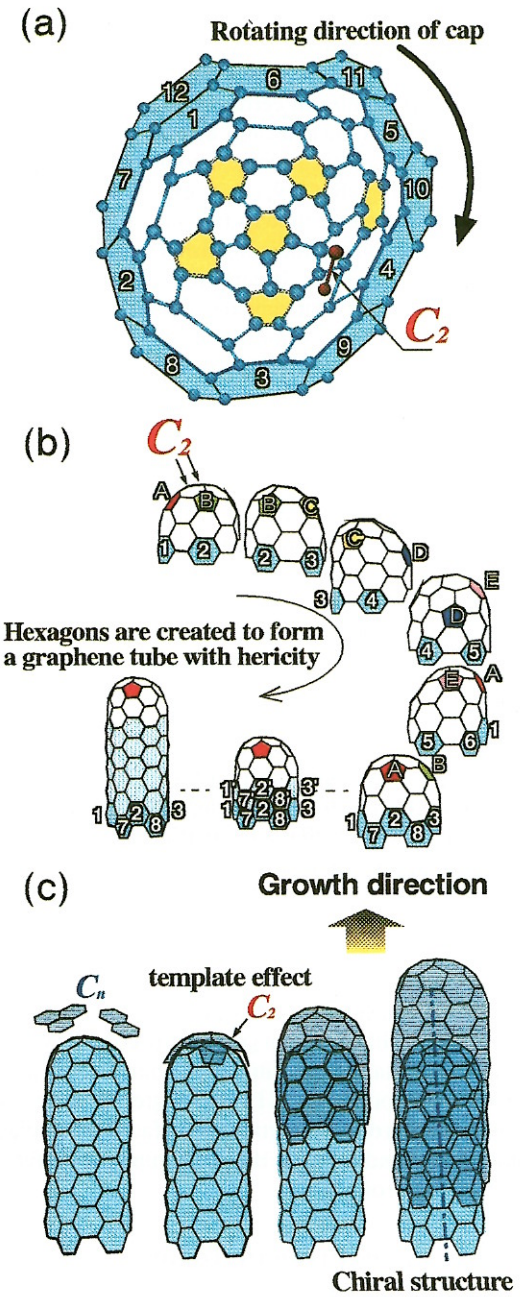

Fig. 10. Growth mechanism proposed for the helical nanotubes (a) and helicity (b), and the model that gives the bridge and laminated tip structure (c).

small closed cage fullerenes. Based on the observation of open-ended tubes, Iijima *et al.*[13] have discussed a plausible alternative way in which such tubules might possibly grow. The closed cap growth mechanism effectively involves the addition of extended chains of sp carbon atoms to the periphery of the asymmetric 6-pentagon cap, of the kind whose Schlegel diagram is depicted in Fig. 10a, and results in a hexagonal graphene cylinder wall in which the added atoms are arranged in a helical disposition[9,11] similar to that observed first by Iijima[1].

It is proposed that during the growth of primary tubule cores, carbon atoms, diameters, and longer linear clusters are continuously incorporated into the active sites, which almost certainly lie in the vicinity of the pentagons in the end caps, effectively creating helical arrays of consecutive hexagons in the tube wall as shown in Fig. 10a,b[9,11]. Sequential addition of 2 carbon atoms at a time to the wall of the helix results in a cap that is indistinguishable other than by rotation[11,12]. Thus, if carbon is ingested into the cap and wholesale rearrangement occurs to allow the new atoms to "knit" smoothly into the wall, the cap can be considered as effectively fluid and to move in a screw-like motion leaving the base of the wall stationary—though growing by insertion of an essentially uniform thread of carbon atoms to generate a helical array of hexagons in the wall. The example shown in Fig. 10a results in a cylinder that has a diameter (ca. 1 nm) and a 22-carbon atom repeat cycle and a single hexagon screw pitch—the smallest archetypal (isolated pentagon) example of a graphene nanotube helix. Though this model generates a tubule that is rather smaller than is usually the case for the PCNTs observed in this study (the simplest of which have diameters > 2–3 nm), the results are of general semi-quantitative validity. Figure 10b,c shows the growth mechanism diagrammatically from a side view. When the tip is covered by further deposition of aromatic layers, it is possible that a templating effect occurs to form the new secondary surface involving pentagons in the hexagonal network. Such a process would explain the laminated or stacked-cup-like morphology observed.

In the case of single-walled nanotubes, it has been recognized recently that transition metal particles play a role in the initial filament growth process[23]. ACNTs and PCNTs have many similarities but, as the vapor-growth method for PCNTs allows greater control of the growth process, it promises to facilitate applications more readily and is thus becoming the preferred method of production.

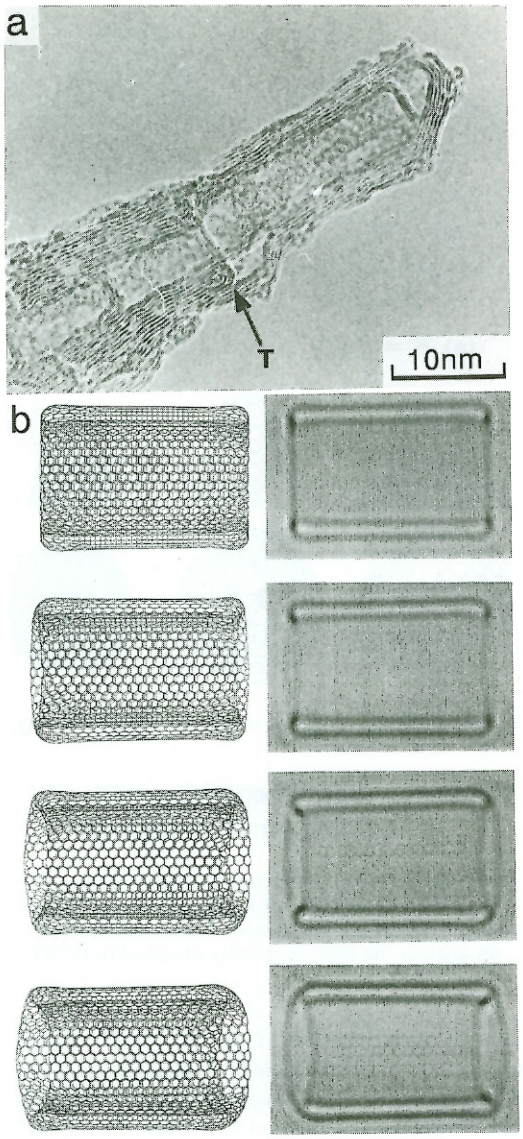

Fig. 11. The sealed tip of a PCNT heat treated at 2800°C with a toroidal structure (T) and, (b) molecular graphics images of archetypal flattened toroidal model at different orientations and the corresponding simulated TEM images.

6. CHARACTERISTIC TOROIDAL AND SPINDLE-LIKE STRUCTURES OF PCNTs

In Fig. 11a is shown an HRTEM image of part of the end of a PCNTs. The initial material consisted of a single-walled nanotube upon which bi-conical spindle-like growth can be seen at the tip. Originally, this tip showed no apparent structure in the HRTEM image at the as-grown state, suggesting that it might consist largely of some form of "amorphous" carbon. After a second stage of heat treatment at 2800°C, the amorphous sheaths graphitize to a very large degree, producing multi-walled graphite nanotubes that tend to be sealed off with caps at points where the spindle-like formations are the thinnest. The sealed-off end region of one such PCNT with a hemi-toroidal shape is shown in Fig. 11a.

In Fig. 11b are depicted sets of molecular graphics images of flattened toroidal structures which are the basis of archetypal double-walled nanotubes[24]. As the orientation changes, we note that the HRTEM interference pattern associated with the rim changes from a line to an ellipse and the loop structures at the apices remain relatively distinct. The oval patterns in the observed and simulated HRTEM image (Fig. 11b) are consistent with one another. For this preliminary investigation a symmetric (rather than helical) wall configuration was used for simplicity. Hemi-toroidal connection of the inner and outer tubes with helical structured walls requires somewhat more complicated dispositions of the 5/6/7 rings in the lip region. The general validity of the conclusions drawn here are, however, not affected. Initial studies of the problem indicated that linking between the inner and outer walls is not, in general, a hindered process.

The toroidal structures show interesting changes in morphology as they become larger—at least at the lip. The hypothetical small toroidal structure shown in Fig. 11b is actually quite smooth and has an essentially rounded structure[24]. As the structures become larger, the strain tends to focus in the regions near the pentagons and heptagons, and this results in more prominent localized cusps and saddle points. Rather elegant toroidal structures with D_{nh} and D_{nd} symmetry are produced, depending on whether the various paired heptagon/pentagon sets which lie at opposite ends of the tube are aligned or are offset. In general, they probably lie is fairly randomly disposed positions. Chiral structures can be produced by off-setting the pentagons and heptagons. In the D_{5d} structure shown in Fig. 11 which was developed for the basic study, the walls are fluted between the heptagons at opposite ends of the inner tube and the pentagons of the outer wall rim[17]. It is interesting to note that in the computer images the localized cusping leads to variations in the smoothness of the image generated by the rim, though it still appears to be quite elliptical when viewed at an angle[17]. The observed image appears to exhibit variations that are consistent with the localized cusps as the model predicts.

In this study, we note that epitaxial graphitization is achieved by heat treatment of the apparently mainly amorphous material which surrounds a single-walled nanotube[17]. As well as bulk graphitization, localized hemi-toroidal structures that connect adjacent walls have been identified and appear to be fairly common in this type of material. This type of infrastructure may be important as it suggests that double walls may form fairly readily. Indeed, the observations suggest that pure carbon rim-sealed structures may be readily produced by heat treatment, suggesting that the future fabrication of stabilized double-walled nanoscale graphite tubes in which dangling bonds have been eliminated is a feasible objective. It will be interesting to prove the relative reactivities of these structures for their possible future applications in nanoscale devices (e.g., as quantum wire supports). Although the curvatures of the rims appear to be quite tight, it is clear from the abundance of loop images observed, that the occurrence of such turnovers between concentric cylinders with a gap spacing close to the standard graphite interlayer spacing is relatively common. Interestingly, the edges of the toroidal structures appear to be readily visible and this has allowed us to confirm the relationship between opposing loops. Bulges in the loops of the kind observed are simulated theoretically[17].

Once one layer has formed (the primary nanotube core), further secondary layers appear to deposit with various degrees of epitaxial coherence. When inhomogeneous deposition occurs in PCNTs, the thickening has a characteristic spindle shape, which may be a consequence of non-carbon impurities which impede graphitization (see below)—this is not the case for ACNTs were growth takes place in an essentially all-carbon atmosphere, except, of course, for the rare gas. These spindles probably include the appropriate number of pentagons as required by variants of Euler's Law. Hypothetical structural models for these spindles are depicted in Fig. 12. It is possible that similar two-stage growth processes occur in the case of ACNTs but, in general, the secondary growth appears to be intrinsically highly epitaxial. This may be because in the ACNT growth case only carbon atoms are involved and there are fewer (non-graphitizing) alternative accretion pathways available. It is likely that epitaxial growth control factors will be rather weak when secondary deposition is very fast, and so thin layers may result in poorly ordered graphitic structure in the thicker sections. It appears that graphitization of this secondary deposit that occurs upon heat treatment may be partly responsible for the fine structure such as compartmentalization, as well as basic tip morphology[17].

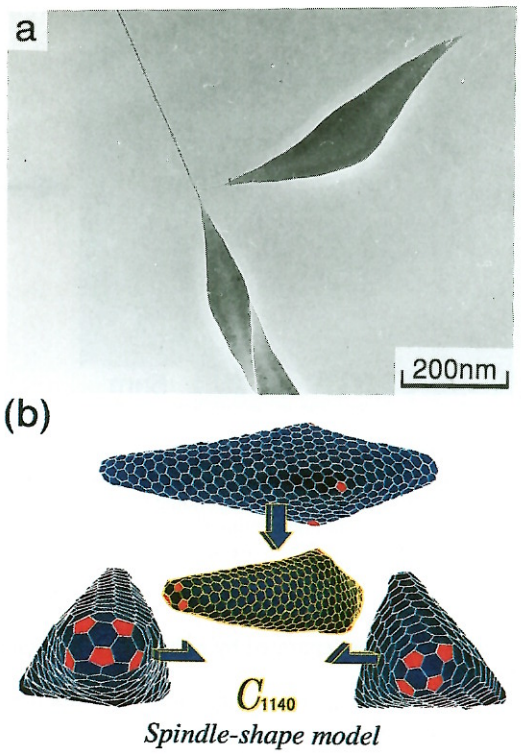

Fig. 12. As-grown PCNTs with partially thickened spindle shape (a) and the proposed structural model for spindle particles including 12 pentagons in hexagon cage (b).

7. VGCFs DERIVED FROM NANOTUBES

In Fig. 13 is shown the 002 lattice images of an "as-formed" very thin VGCF. The innermost core diameter (ca. 20 nm as indicated by arrows) has two layers; it is rather straight and appears to be the primary nanotube. The outer carbon layers, with diameters ca. 3–4 nm, are quite uniformly stacked parallel to the central core with 0.35 nm spacing. From the difference in structure as well as the special features in the mechanical strength (as in Fig. 7) it might appear possible that the two intrinsically different types of material

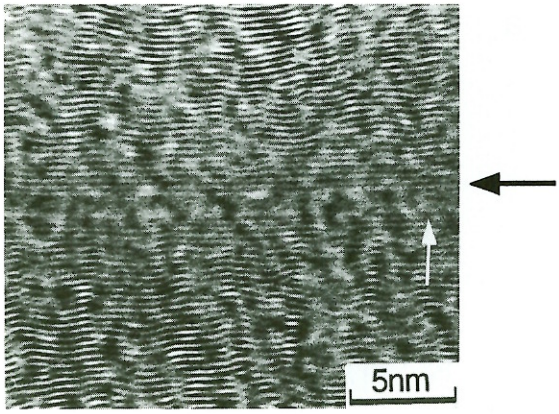

Fig. 13. HRTEM image of an as-grown thick PCNT. 002 lattice image demonstrates the innermost hollow core (core diam. 2.13 nm) presumably corresponding to the "as-formed" nanotube. The straight and continuous innermost two fringes similar to Fig. 5 are seen (arrow).

involved might be separated by pulverizing the VGCF material.

In Fig. 14a, a ca. 10 μm diameter VGCF that has been broken in liquid nitrogen is depicted, revealing the cylindrical graphitic nanotube core with diameter of ca. 10 nm (white arrow), observed by field emission scanning electron microscopy (FE-SEM)[25]. It is, thus, suggested that at least some of the VGCFs start as nanotube cores, which act as a substrate for subsequent thickening by deposition of secondary pyrolytic carbon material, as in the catalytically primarily grown hollow fiber. In Fig. 14b is also shown the TEM image corresponding to the extruded nanotube from a very thin fiber. It is clearly observed that the exposed nanotube is continuing into the fiber as a central hollow core, as indicated by the white arrow in the figure. It is interesting that, as indicated before (in Fig. 14a), the core is more flexible than the pyrolytic part, which is more fragile.

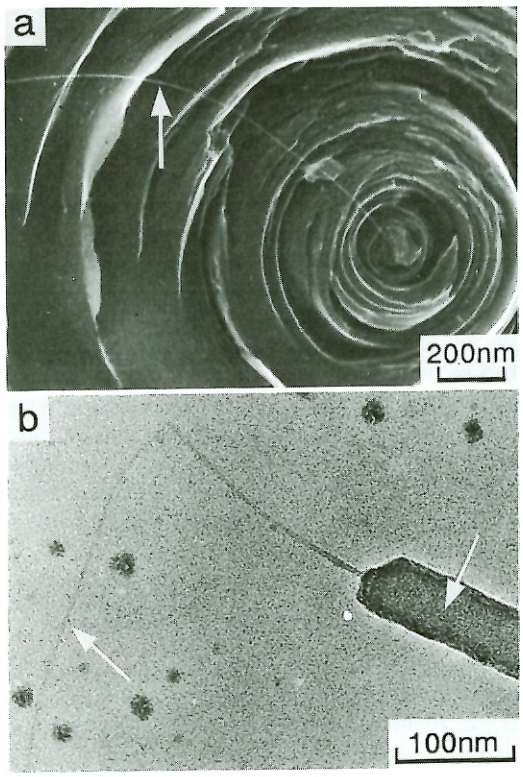

Fig. 14. PCNTs (white arrow) appeared after breakage of VGCF, (a) FE-SEM image of broken VGCF, cut in liquid nitrogen and (b) HRTEM image showing the broken part observed in very thin VGCF. The nanotube is clearly observed and this indicates that thin VGCF grow from nanometer core by thickening.

8. CONCLUSION

Pyrolytic carbon nanotubes (PCNTs), which grow during hydrocarbon pyrolysis, appear to have structures similar to those obtained by arc/discharge techniques using graphite electrodes (ACNTs). The PCNTs tend to exhibit a characteristic thickening feature due to secondary pyrolytic carbon deposition. Various tip morphologies are observed, but the one most frequently seen has a 20° opening angle, suggesting that, in general, the graphene conical tips possess a cluster of five pentagons that may be actively involved in tube growth. PCNTs with spindle-like shapes and that have conical caps at both ends are also observed, for which a structural model is proposed. The spindle-like structures observed for the secondary growth thickening that occurs in PCNTs may be a consequence of the lower carbon content present in the growth atmosphere than occurs in the case of ACNT growth. Possible structural models for these spindles have been discussed. The longitudinal growth of nanotubes appears to occur at the hemi-spherical active tips and this process has been discussed on the basis of a closed cap mechanism[9,11]. The PCNTs are interesting, not only from the viewpoint of the fundamental perspective that they are very interesting giant fullerene structures, but also because they promise to be applications in novel strategically important materials in the near future. PCNT production appears, at this time, more readily susceptible to process control than is ACNT production and, thus, their possible value as fillers in advanced composites is under investigation.

Acknowledgements—Japanese authors are indebted to M. S. Dresselhaus and G. Dresselhaus of MIT and to A. Oberlin of Laboratoire Marcel Mathieu (CNRS) for their useful discussions and suggestions. HWK thanks D. R. M. Walton for help and the Royal Society and the SERC (UK) for support. Part of the work by ME is supported by a grant-in-aid for scientific research in priority area "carbon cluster" from the Ministry of Education, Science and Culture, Japan.

REFERENCES

1. S. Iijima, *Nature* **354**, 56 (1991).
2. H. W. Kroto, J. R. Heath, S. C .O'Brien, R. F. Curl, and R. E. Samlley, *Nature* **318**, 162 (1985).

3. T. W. Ebbesen and P. M. Ajayan, *Nature* **358**, 220 (1992).
4. M. Endo, H. Fijiwara, and E. Fukunaga, *18th Meeting Japanese Carbon Society*, (1991) p. 34.
5. M. Endo, H. Fujiwara, and E. Fukunaga, *2nd C60 Symposium in Japan*, (1992) p. 101.
6. M. Endo, K. Takeuchi, S. Igarashi, and K. Kobori, *19th Meeting Japanese Carbon Society*, (1992) p. 192.
7. M. Endo, K. Takeuchi, S. Igarashi, K. Kobori, and M. Shiraishi, *Mat. Res. Soc. Spring Meet* (1993) p.S2.2.
8. M. Endo, K. Takeuchi, S. Igarashi, K. Kobori, M. Shiraishi, and H. W. Kroto, *Mat. Res. Soc. Fall Meet.* **G2.1** (1994).
9. M. Endo, K. Takeuchi, S. Igarashi, K. Kobori, M. Shiraishi, and H. W. Kroto, *J. Phys. Chem. Solids* **54**, 1841 (1993).
10. M. Endo, *Chemtech* **18**, 568 (1988).
11. M. Endo and H. W. Kroto, *J. Phys. Chem.* **96**, 6941 (1992).
12. H. W. Kroto, K. Prassides, R. Taylor, D. R. M. Walton, and M. Endo, *International Conference Solid State Devices and Materials of The Japan Society of Applied Physics* (1993), p. 104.
13. S. Iijima, *Mat. Sci. Eng.* **B19**, 172 (1993).
14. P. M. Ajayan, T. W. Ebbesen, T. Ichihashi, S. Iijima, K. Tanigaki, and H. Hiura, *Nature* **362**, 522 (1993).
15. M. S. Dresselhaus, G. Dresselhaus, K. Sugihara, I. L. Spain, H. A. Goldberg, In *Graphite Fibers and Filaments*, (edited by M. Cardona) pp. 244–286. Berlin, Springer.
16. J. S. Speck, M. Endo, and M. S. Dresselhaus, *J. Crystal Growth* **94**, 834 (1989).
17. A. Sarkar, H. W. Kroto, and M. Endo (in preparation).
18. H. Hiura, T. W. Ebbesen, J. Fujita, K. Tanigaki, and T. Takada, *Nature* **367**, 148 (1994).
19. M. Ge and K. Sattler, *Mat. Res. Soc. Spring Meet.* **S1.3**, 360 (1993).
20. G. Ulmer, E. E. B. Cambel, R. Kuhnle, H. G. Busmann, and I. V. Hertel, *Chem. Phys. Letts.* **182**, 114 (1991).
21. S. W. McElvaney, M. N. Ross, N. S. Goroff, and F. Diederich, *Science* **259**, 1594 (1993).
22. R. Saito, G. Dresselhaus, M. Fujita, and M. S. Dresselhaus, *4th NEC Symp. Phys. Chem. Nanometer Scale Mats.* (1992).
23. S. Iijima, *Gordon Conference on the Chemistry of Hydrocarbon Resources*, Hawaii (1994).
24. A. Sarker, H. W. Kroto, and M. Endo (to be published).
25. M. Endo, K. Takeuchi, K. Kobori, K. Takahashi, and H. W. Kroto (in preparation).